Optimal UAV Route Planning for Coverage Search of Stationary Target in River

Peng Yao, Zexiao Xie, and Ping Ren

***Abstract*— In this brief, we focus on the offline route planning of unmanned aerial vehicle (UAV) for the coverage search mission in a river region. Given the prior likelihood distribution of area importance, this brief aims to generate UAV feasible routes which maximize the cumulative probability of finding a single and stationary target within the required time. First, Gaussian mixture model is used to approximate the prior likelihood distribution, and several river segments with high detection probability corresponding to Gaussian components can be extracted. With the consideration of quantified factors, the river subregions are prioritized by the approximation insertion method and then allocated to UAVs. Moreover, to meet the terminal time constraint, the so-called positive/negative greedy method is proposed to expand or contract waypoints. Finally, the performance of our proposed algorithm is evaluated by simulations on a real river map, and the results verify its good performance in various scenarios.**

***Index Terms*— Coverage search, cumulative probability, river region, route planning, unmanned aerial vehicle (UAV).**

I. Introduction

UNMANNED aerial vehicle (UAV) equipped with airborne sensor (e.g., camera and sonar) is increasingly employed in various applications such as mapping, surveillance, or perimeter patrol [1]–[4]. Particularly, UAV is suitable for the coverage task required in target search application, as it has wider field of view and more flexible maneuverability than ground or water vehicle. Suppose a person was lost in wild or a ship was sinking into the sea, the probability of survival would decrease rapidly as time went on. In this time-sensitive case, UAV is demanded to detect the area of interest efficiently in order to find the target as soon as possible. Therefore, the coverage search mission can be modeled as an optimization problem of planning feasible routes, along which the sensor footprint covers the important area in order to maximize the cumulative detection probability within limited flight time [5]. Different from traditional route planning tasks which generate obstacle avoidance routes from start point to destination [6], [7], this mission is much more complicated due to the demand of providing coverage of possibly important areas. In the past decades, researchers have presented various search strategies which could be roughly divided into two categories [8].

The first kind belongs to the exhaustive strategy, i.e., UAV exhaustively sweeps the region if no prior knowledge such as target likelihood distribution can be referred to. For example, some geometric methods including Zamboni or spiral search are employed to achieve the uniform coverage of region [9]–[11]. In [12], the space is discretized into nodes with adjacent edges of a graph, and consequently, a graph-search-based strategy is formulated. As the region is entirely covered without heuristic, however, the exhaustive strategy is obviously inefficient if subareas of no interest exist.

Given the prior likelihood distribution of target, the second kind (including mathematical or heuristic methods) first discretizes the space into cells or particles attached with values and then plans efficient motions of UAV visiting high-value areas but ignoring low-likelihood regions, which is based on the objective function such as the short-term detection probability or the mean time to detection [5], [13]. Lanillos *et al.* [14] present a real-time receding horizon controller (RHC) in continuous action space, using a decentralized gradient-based optimization algorithm where the expected observation is taken as an estimate of future. Hu *et al.* [15] utilize a consensus-like distributed scheme to fuse the probability map of each UAV based on Bayesian rule and then design the coverage control, i.e., optimal configuration of all agents. Other search strategies include but are not limited to probabilistic decision-making method [16] and mixed-integer linear programming (MILP) [17]. However, most methods make a tradeoff between the length of time horizon and the calculation cost, so they may suffer from local minimums, i.e., the suboptimal routes may be finally obtained. Hence, our previous work extracts high-value subregions by Gaussian mixture model (GMM) and plans UAV motions heuristically using concurrent RHC through the parameterized spaces at different levels of resolution [18].

The above methods can only be used in a 2-D wide space. This brief, however, will focus on a river region modeled as one kind of abstract space subject to geographical constraints. To the best of the authors' knowledge, there are few relevant works about the river coverage search, and the common solution is entirely sweeping along the river or directly detecting the subspaces of interest by UAV or surface vessel without quantified heuristic [19]. Actually, the river coverage search mission is similar to the well-studied road-network search route planning problem [20], [21], once the river subregions of interest are extracted quantitatively and taken

Manuscript received October 17, 2017; revised November 17, 2017; accepted December 2, 2017. Date of publication December 22, 2017; date of current version February 8, 2019. Manuscript received in final form December 3, 2017. This work was supported in part by the China Postdoctoral Science Foundation under Grant 2017M622278, in part by the Fundamental Research Funds for the Central Universities under Grant 201713046, and in part by the National Natural Science Foundation of China under Grant 61571408 and Grant 51409237. Recommended by Associate Editor A. G. Aghdam. *(Corresponding author: Peng Yao.)*

The authors are with the College of Engineering, Ocean University of China, Qingdao 266100, China (e-mail: yaopenghappy@163.com; xiezexiao@ouc.edu.cn; robotics@ouc.edu.cn).

Color versions of one or more of the figures in this paper are available online at http://ieeexplore.ieee.org.

Digital Object Identifier 10.1109/TCST.2017.2781655

as connected or unconnected roads. As the abstract geography restricts UAV motion directions, the traditional strategies are usually inefficient for the road-network search. Hence, some methods converted from standard problems or improved from traditional search strategies are proposed. Oh *et al.* [21] formulate it as an extended Chinese postman problem (CPP) without constraining UAV coverage to graph's connectivity but adding Dubins motion to meet UAV physical constraints and solve the problem by MILP and approximation approach, respectively. Dille and Singh [22] generate global coverage patterns on road networks in sparse environments by solving the sweeping generalized traveling salesman problem (TSP). Relying on short-term locational optimization, Meng *et al.* [23] propose a coverage control formulation for multi-UAV search on a roadmap of urban environment, and UAVs will be quickly separated on different roads within minutes. Other methods are available in [24]–[26]. However, most of the state-of-the-art methods ignore the target probability distribution. Even if some methods [23] take into account the relevant knowledge, UAVs may get stuck in the local minimums with short-time horizon.

Based on the above analysis, this brief studies the UAV route planning problem for searching a single and stationary target with prior likelihood of existence in a river region. With proper expression, GMM is first used to describe the likelihood distribution of target and extract the high-value river subregions. Hence, other areas of no interest will be neglected, but the parameterized regions attached with high probability will be chosen and swept by UAVs in a sorted sequence, which is achieved by the approximation insertion (AI) approach for its simple numerical calculation. The above two strategies will ensure UAV to collect sufficient detection payoff effectively. In addition, the so-called positive/negative greedy method is proposed to meet the terminal time constraint.

The remaining brief is organized as follows. Section II formulates the river coverage search problem in detail. Section III describes the solution framework. Section IV gives the simulation results. The conclusion is drawn in Section V.

II. Problem Formulation

A. UAV Model

The simplified UAV model is used [27]

$$\begin{bmatrix} \dot{x} \\ \dot{y} \\ \dot{\theta} \end{bmatrix} = \begin{bmatrix} V\cos\theta \\ V\sin\theta \\ \omega \end{bmatrix} \tag{1}$$

where (x, y) is UAV's inertial position, V the speed, θ the heading angle, and ω the yaw rate satisfying $|\omega| \le \omega_{\max}$. The minimum turning radius is defined as $R_{\min} = V/\omega_{\max}$. Besides, each UAV flies at different heights for collision avoidance. To ensure the sampling accuracy, UAV's speed when flying above the river region is assumed to be less than (e.g., half of) that during the cruise (i.e., transferring among river segments).

B. Framework of Coverage Search in a River Region

In this brief, N_u UAVs equipped with gimbaled cameras are demanded to search the target such as sinking ship or missing person in a river. Fig. 1 shows the compressed Google map of Wulong river, Shandong Province, China. Assume that the line of sight of sensor always aims straight down even if UAV performs rolling maneuvers, and the river is taken as a curve subject to UAV physical constraints. It is then divided into $M = L/L_s$ uniform parts or cells with respect to forward distance s, where L denotes the river length and L_s the cell length. Hence, each cell m with center point (x_m, y_m) can be expressed by $s_m = m \cdot L_s$ directly, which transforms the 2-D problem into 1-D. Besides, we assume UAV is exactly above the cell center when sweeping river and flies to adjacent cell during one interval of time.

Fig. 1. Google map of Wulong river from GIS satellite data. Available at: www.google.cn/maps/@36.7183512,120.7271107,13939m.

The case of searching a single and stationary target is considered here. The prior likelihood distribution is assumed to be already known with attached values $p(\boldsymbol{x}_0^m|z_0^m) \in [0, 1]$, where vector $\boldsymbol{x}_0^m$ means the position of cell m and z_0^m denotes whether UAV detects the cell or not (1 or 0). The probability distribution map should satisfy

$$\sum_{m=1}^{M} p\left(\boldsymbol{x}_0^m|z_0^m\right) = 1. \tag{2}$$

At time $t(t = 1, 2, \ldots, T)$, using Bayesian rule where all the historical observations $z_{1:t}^m = \{z_1^m, \ldots, z_t^m\}$ are independent, the target probability $p(\boldsymbol{x}_t^m|z_{1:t}^m)$ is updated as follows [5]:

$$p\left(\boldsymbol{x}_t^m|z_{1:t}^m\right) = \lambda \cdot p\left(\boldsymbol{x}_{t-1}^m|z_{1:t-1}^m\right) \cdot \left(1 - g\left(z_t^m|\boldsymbol{x}_t^m\right)\right) \tag{3}$$

where $\boldsymbol{x}_t^m$ and $\boldsymbol{x}_{t-1}^m$ are the same, λ is the normalization factor defined as $\lambda = 1/\sum_{m=1}^{M}(p(\boldsymbol{x}_{t-1}^m|z_{1:t-1}^m) \cdot (1 - g(z_t^m|\boldsymbol{x}_t^m)))$, $p(\boldsymbol{x}_{t-1}^m|z_{1:t-1}^m)$ the target probability at time $t-1$, and $g(z_t^m|\boldsymbol{x}_t^m)$ the new conditional observation likelihood. If UAV is over cell m at time t (denoted as $z_t^m = 1$), a new detection will occur with sensor detection probability $g_s \in (0, 1]$. Otherwise, no detection is available. Hence, $g(z_t^m|\boldsymbol{x}_t^m)$ is defined as

$$g(z_t^m|\boldsymbol{x}_t^m) = \begin{cases} g_s & \text{if } z_t^m = 1 \\ 0 & \text{otherwise.} \end{cases} \tag{4}$$

The conditional probability $\bar{D}_t$, that the target is not detected during one observation, is equal to the volume of the surface formed by multiplying the target probability and

"no detection" probability

$$\bar{D}_t = \sum_{m=1}^{M} \left(p\left(\boldsymbol{x}_{t-1}^m | z_{1:t-1}^m\right) \cdot \left(1 - g\left(z_t^m | \boldsymbol{x}_t^m\right)\right)\right). \tag{5}$$

Actually, $\bar{D}_t$ is the sum of the updated probability distribution surface but before normalization process in (3). As the conditions $\sum_{m=1}^{M} p(\boldsymbol{x}_{t-1}^m | z_{1:t-1}^m) = 1$ and $1 - g(z_t^m | \boldsymbol{x}_t^m) \leq 1$ hold, $\bar{D}_t$ is always less than 1. As each observation is conditionally independent of others, the joint probability of failing to detect target until time t is obtained

$$\bar{D}_{1:t} = \prod_{i=1}^{t} \bar{D}_i. \tag{6}$$

Therefore, the probability that the target has been detected among t steps is

$$D_{1:t} = 1 - \bar{D}_{1:t}. \tag{7}$$

To distinguish it from the conditional detection probability $1 - \bar{D}_t$, $D_{1:t}$ is called the cumulative detection probability at time t. Due to the condition $\bar{D}_t < 1$, $D_{1:t}$ will increase toward 1 as $t \to \infty$. Actually $D_{1:t}$ can be expressed by $D_{1:t} = \sum_{i=1}^{t} D_i$, and D_i is the probability of getting detected for the first time

$$D_i = \bar{D}_{1:i-1} \cdot (1 - \bar{D}_i). \tag{8}$$

Let $\phi = \{\phi_1, \ldots, \phi_{N_u}\}$ be the sample routes of N_u UAVs among T time steps, and Φ be the route set. Then, the cumulative detection probability $D_{1:T}(\phi)$ can be computed by (7). The optimal UAV route planning for coverage search can be formulated as an optimization problem, which aims to find the routes obtaining the maximum detection payoff

$$\phi^* = \arg\max_{\phi \in \Phi} D_{1:T}(\phi). \tag{9}$$

III. UAV Route Planning for River Coverage Search

As the probability distribution map is assumed to be known, the heuristic strategies using prior knowledge are certainly more efficient than the traditional exhaustive methods (e.g., sweeping the river mechanically). First, the river region is quantitatively described by GMM, and several subregions representing high-value clusters of probability volume are extracted. Then, these connected or unconnected river segments are prioritized approximately using AI method and allocated to multi-UAVs. Therefore, the routes following the prioritized river subregions as well as the routes transferring among subregions compose the whole path. Besides, to meet the terminal time constraint, the positive/negative greedy method is presented to expand or contract waypoints of routes.

A. Extraction of River Subregions

There usually exist several high-value clusters of prior likelihood distribution in a river region. GMM can be utilized to approximate the probability distribution map and extract the subregions corresponding to these clusters with Gaussian probability density functions [18], [28].

First, N data points ($N \geq M$) are chosen to form the training samples, each of which is located at cell center. To reflect the region features objectively, the number of data points located at each cell must be proportional to the prior probability

$$N_m = p\left(\boldsymbol{x}_0^m | z_0^m\right) \cdot N. \tag{10}$$

Suppose K Gaussian components $G_k(s)$ ($k = 1, \ldots, K$) with weighs α_k compose the mixture model, which should satisfy

$$\sum_{k=1}^{K} \alpha_k = 1. \tag{11}$$

As the river can be transformed into 1-D by taking the forward distance s as independent variable, the probability density function of each Gaussian model is defined

$$G_k(s) = \frac{1}{\sqrt{2\pi}\sigma_k} \exp\left(-\frac{(s - u_k)^2}{2\sigma_k^2}\right) \tag{12}$$

where σ_k is the standard deviation (SD) and u_k the mean value. The weighted sum of Gaussian models should represent the prior target likelihood distribution as accurately as possible

$$p\left(\boldsymbol{x}_0^m | z_0^m\right) \approx \sum_{k=1}^{K} \alpha_k G_k(s). \tag{13}$$

To achieve good representation or approximation as (13), the parameters of Gaussian component, i.e., α_k, σ_k, and u_k should be estimated. First, the K-means method is adopted to generate K initial clusters, and then, the expectation maximization approach is used to iteratively estimate the parameters by taking expectation and maximization steps until the convergence condition is met. In this brief, three dynamic adaptive strategies are also introduced into the iteration step, aiming to eliminate, merge, or decompose Gaussian models. The number K will be flexible in accordance with the scenario, which in the end is probably unequal to the initial value. First, for any Gaussian component attached with very small coefficient (e.g., $\alpha_k < 0.01$) and far away from others, for example

$$|u_k - u_p| \gg (1/(K-1)(K-2)) \sum_{\substack{i=1 \\ i \neq k}}^{K} \sum_{\substack{j=1 \\ j \neq k}}^{K} |u_i - u_j| \quad \forall p \in \{1, \ldots, K\}, \quad p \neq k$$

it can be eliminated as a low-value or even noise model. Second, when the overfitting event happens, i.e., two low-weight components ($0.01 < \alpha_k < 0.05, 0.01 < \alpha_p < 0.05$) are too close ($|u_k - u_p| < \sigma_k + \sigma_p$), they can be merged into one model. Third, when the underfitting event happens, i.e., a Gaussian component has large weight ($\alpha_k > 0.1$) and SD ($\sigma_k > L/2$), it should be divided into two models.

Based on the estimation results, the river segments can be extracted. The corresponding area of each estimated model

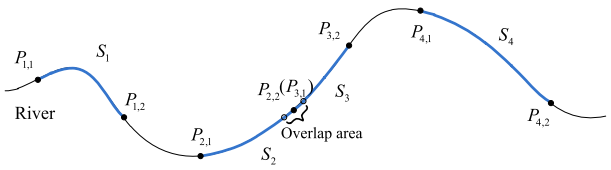

Fig. 2. Illustration of extracted river subregions.

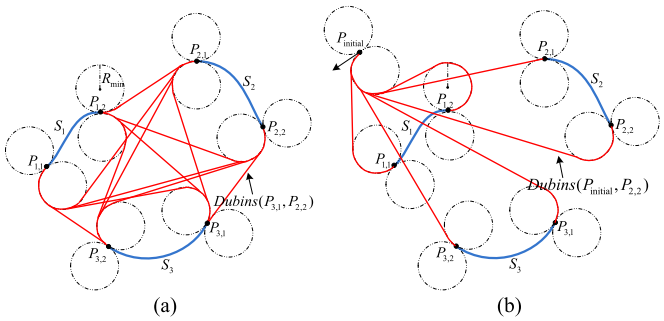

Fig. 3. Illustration of synthesized graph using Dubins connections. (a) Connecting nodes. (b) Connecting UAV initial point and nodes.

is the river interval under standard Gaussian surface within two SDs (the volume of probability is 95.4%), denoted as $S_k = (u_k - 2\sigma_k, u_k + 2\sigma_k)$. Hence, the center u_k, length $4\sigma_k$, boundary points $P_{k,1} = u_k - 2\sigma_k$ and $P_{k,2} = u_k + 2\sigma_k$, and the weight α_k of each subregion are determined quantitatively.

Fig. 2 shows the extracted river subregions (blue curves). Note that there are overlapping subregions S_2 and S_3, which can be simplified as connected ones by taking the midpoint of overlap area as the common boundary point (i.e., $P_{2,2} = P_{3,1}$).

B. Prioritization and Allocation of River Subregions

Once the river segments are extracted by GMM, UAVs should follow or sweep these river segments sequentially in order to obtain the maximum detection payoff. Therefore, the parameterized subregions should be prioritized and allocated.

1) Evaluation Factors: On the basis of extracted river subregions, three evaluation factors including region-transferring time, region-sweeping time, and region-sweeping reward are used.

A fully connected graph is first synthesized. This graph contains K elements, i.e., river curve segments $\{S_1, \ldots, S_K\}$, and each segment is attached with two nodes (i.e., boundary points $P_{k,1}$ and $P_{k,2}$) along the direction of river curve. Then, this graph is formed by connecting each node to all the other nodes except its partner, and the corresponding edge is obtained by Dubins method, which proves to be the shortest path between points under UAV motion constraints [29]. Besides, a graph by connecting UAV initial point P_{initial} and any boundary points is constructed. If the endpoint P_{end} exists, a graph by connecting nodes and endpoint can be generated similarly. Fig. 3 shows the generated graph containing three river subregions, where the blue curves represent the river subregions while the red curves are the node-to-node Dubins paths. Then, the region-transferring time between any two nodes is calculated

$$T(P_{i,p}, P_{j,q}) = \begin{cases} \lambda_1 \cdot \text{Dubins\_cost}(P_{i,p}, P_{j,q}) & \text{if } i \neq j \\ +\infty & \text{otherwise} \end{cases} \tag{14}$$

where $p, q \in \{1, 2\}$, $i, j \in \{1, \ldots, K\}$, $\text{Dubins\_cost}(P_{i,p}, P_{j,q})$ means the length of Dubins path from node $P_{i,p}$ to $P_{j,q}$, and the penalty function is also introduced in order to avoid transferring between the partner nodes or the same nodes. Then, the region-transferring time matrix with size $2K \times 2K$ can be taken as the database for segment sequencing. Besides, we can calculate the region-transferring time between initial point and nodes, i.e., $T(P_{\text{initial}}, P_{j,q})$, or that between nodes and endpoint, i.e., $T(P_{i,p}, P_{\text{end}})$ in the same way.

The region-sweeping time is actually the time spent on flying over the river subregion. As the length of each river segment is $4\sigma_k$, its region-sweeping time can be defined as

$$C_k = \lambda_2 \cdot 4\sigma_k. \tag{15}$$

As λ_1 and λ_2 are the coefficients of region-transferring time and region-sweeping time, respectively, their relationship is negatively correlated with that between UAV speeds.

The volume of probability under the standard Gaussian function of each river subregion is 95.4% with the coefficient α_k. Hence, the region-sweeping reward is approximate to

$$R_k = 0.954\alpha_k. \tag{16}$$

2) AI Method: In essence, the subregion prioritization can be taken as a generalized TSP or CPP. However, this brief considers not only the distances of region-sweeping or region-transferring routes under UAV motion constraints, but also the predicted detection reward of each subregion.

The case that single UAV sweeps K subregions with no endpoint is first discussed here. If the sequence of subregions is $l_1, \ldots, l_K$ with the corresponding mark of subregion-inward point (i.e., the entrance point of sweeping river subregion) $n_1, \ldots, n_K \in \{1, 2\}$, the alternative region-transferring and region-sweeping routes will combine the whole path

$$\begin{aligned} \text{Path} = \{&\text{Dubins}(P_{\text{initial}}, P_{l_1,n_1}), S_{l_1}(P_{l_1,n_1}, P_{l_1,3-n_1}), \\ &\text{Dubins}(P_{l_1,3-n_1}, P_{l_2,n_2}), S_{l_2}(P_{l_2,n_2}, P_{l_2,3-n_2}), \\ &\ldots, \text{Dubins}(P_{l_{K-1},3-n_{K-1}}, P_{l_K,n_K}), \\ &S_{l_K}(P_{l_K,n_K}, P_{l_K,3-n_K})\}. \end{aligned} \tag{17}$$

Our objective is to obtain the maximum cumulative detection probability, so the subregion prioritization can be modeled as the following optimization problem:

$$\max J = \frac{R_{l_1}}{T(P_{\text{initial}}, P_{l_1,n_1}) + C_{l_1}} + \sum_{k=2}^{K} \frac{R_{l_k}}{T(P_{l_{k-1},3-n_{k-1}}, P_{l_k,n_k}) + C_{l_k}}. \tag{18}$$

As shown in (18), three evaluation factors determine the priority index of each subregion. The subregion with larger detection reward and shorter distance will have higher priority certainly. Due to the high efficiency, the AI method

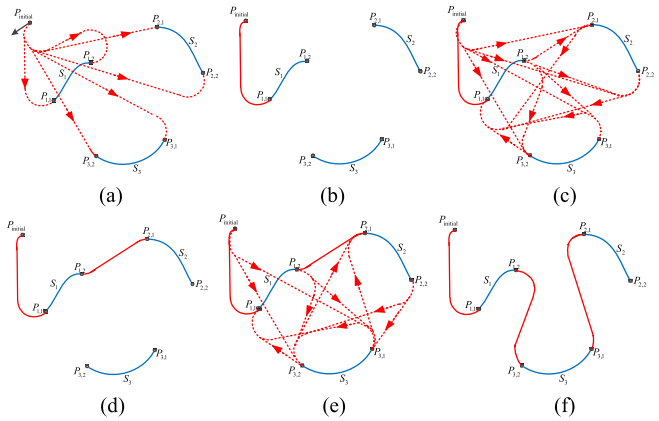

Fig. 4. Illustration of AI method. (a) Find the best edge. (b) First time (choose S_1). (c) Find the best edge. (d) Second time (S_2 is stacked after S_1). (e) Find the best edge. (f) Third time (S_3 is inserted between S_1 and S_2).

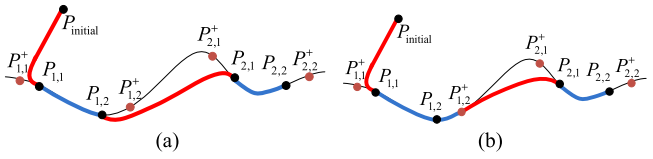

Fig. 5. Process of expanding waypoints. (a) Choose expanded waypoints. (b) Update the route ($P^+_{1,2}$ is added).

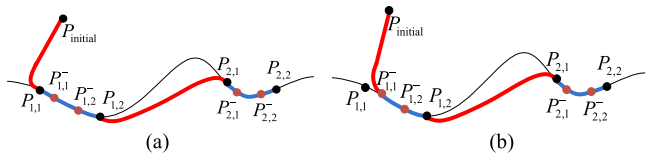

Fig. 6. Process of contracting waypoints. (a) Choose contracted waypoints. (b) Update the route ($P_{1,1}$ is deleted).

is improved here to heuristically prioritize subregions using the comprehensive priority index, rather than only the path length in [21] and [30]. It produces a suboptimal tour less than twice the optimal regardless of the number of nodes, with the calculation time only proportional to the square of nodes. The process of AI is as follows. At each iteration, we compute the priority indices of all the cases that any subregion from the remaining set is inserted into or stacked after the set of already prioritized subregions and then choose the case with maximum value progressively. The above procedures repeat K times until the whole tours are constructed. Fig. 4 illustrates a simple example of prioritizing three subregions. Note that when the subregion S_3 is inserted, the original edge Dubins($P_{1,2}$, $P_{2,1}$) is replaced by new edges Dubins($P_{1,2}$, $P_{3,2}$) and Dubins($P_{3,1}$, $P_{2,1}$).

If multi-UAVs perform search mission, the river segments should first be allocated to UAVs, aiming to simplify and decouple the cooperative control problem. Then, each UAV only needs to visit its allocated subregions in sequence as mentioned earlier. Suppose that the allocated and prioritized subregions of UAVi are denoted as $\boldsymbol{A}_i$, and its corresponding evaluation index J_i is obtained by (18). Considering the total reward and team balance, the allocation problem is modeled as

$$\max J = \rho_1 \sum_{i=1}^{N_u} J_i + \rho_2 \max_{i,j\in\{1,\ldots,N_u\}} \{|J_i - J_j|\}. \tag{19}$$

Each subregion is only allocated to one UAV for collision avoidance, i.e., the following constraints should be met:

$$\begin{aligned} \boldsymbol{A}_i \cap \boldsymbol{A}_j &= \emptyset, \quad \forall i, j \in \{1,\ldots,N_u\},\ i \neq j \\ \boldsymbol{A}_i &\neq \emptyset, \quad \forall i \in \{1,\ldots,N_u\} \\ \bigcup_{i=1}^{N_u} \boldsymbol{A}_i &= \{1,\ldots,K\}. \end{aligned} \tag{20}$$

The auction algorithm is employed here to solve the allocation problem quickly.

C. Terminal Time Constraint

In this brief, UAVs are demanded to finish the task at given mission time T_{given}. However, the total flight time T_{path} along the planned path by (17) is usually not equal to mission time. Hence, the positive/negative greedy method is proposed to modify routes by expanding or contracting waypoints.

If T_{path} is smaller than T_{given}, waypoints should be expanded of course. When it comes to river segments $\{S_1,\ldots,S_K\}$, there are $2K$ boundary points $\{P_{1,1}, P_{1,2},\ldots,P_{K,1}, P_{K,2}\}$ in order, and all the possibly expanded waypoints, i.e., the next points outward along river are denoted as $\{P^+_{1,1}, P^+_{1,2},\ldots,P^+_{K,1}, P^+_{K,2}\}$. The one with the maximum probability is chosen as expanded waypoint

$$\begin{aligned} &P^+_{k*,q*} \\ &\quad = \arg\max \left(p\left(P^+_{k,q}|z_{1:t}\right)\right), \quad \forall k \in \{1,\ldots,K\},\ q \in \{1,2\}. \end{aligned} \tag{21}$$

The transferring path is also updated. Hence, T_{path} increases and the above procedures repeat until $T_{\text{path}} = T_{\text{given}}$.

If T_{path} is larger than T_{given}, waypoints should be contracted. From all the boundary points, the one with the minimum existence probability of target is chosen

$$\begin{aligned} &P_{k*,q*} \\ &\quad = \arg\min \left(p\left(P_{k,q}|z_{1:t}\right)\right), \quad \forall k \in \{1,\ldots,K\},\ q \in \{1,2\}. \end{aligned} \tag{22}$$

Then, $P_{k*,q*}$ is deleted, and its next point inward along the river, denoted as $P^-_{k*,q*}$, is taken as the new boundary point of corresponding river segment. Hence, T_{path} decreases and the above procedures repeat until $T_{\text{path}} = T_{\text{given}}$.

Figs. 5 and 6 illustrate the process of expanding and contracting waypoints, respectively, where the red curves mean the region-transferring routes and the blue curves denote the region-sweeping routes. With greedy consideration of detection payoff, the time-constrained routes will be determined very quickly.

Although the time constraint can be met as above, UAV may spend most time transferring between subregions when the mission time is very short. In this case, the subregions with higher detection value should be preferred while others should be abandoned or skipped in order to enhance the efficiency. First, the time that UAV sweeps the former $1,\ldots,K$ subregions, denoted as $T_{\text{path}_1},\ldots,T_{\text{path}_K}$, are calculated, respectively. Then, the one which is closest to the mission time is

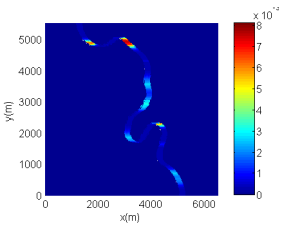

Fig. 7. Prior likelihood distribution map (note that the river's width is increased for clarity in this figure and Fig. 10).

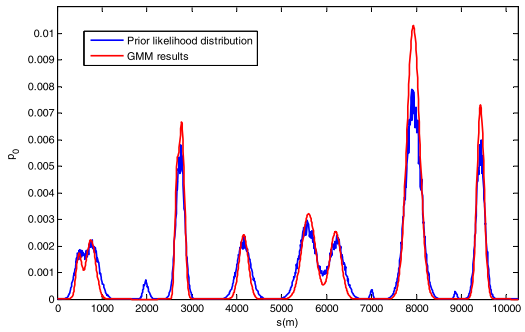

Fig. 8. GMM approximation results.

obtained

$$k^* = \arg \min_{k \in \{1,\ldots,K\}} |T_{\text{path}_k} - T_{\text{given}}|. \tag{23}$$

The first k^* subregions are chosen, among which the positive/negative greedy method is then utilized.

IV. Simulation

In order to evaluate the performance of our proposed GMM-AI method, some simulations are performed on the river map of Fig. 1, conducted in MATLAB on a computer with 64-b Intel Core i5-7200U CPU with 2.5-GHz frequency. The first work shows the average results with different numbers of UAVs using GMM-AI. Then, we compare GMM-AI with some other approaches to highlight its efficiency. Unless otherwise specified, the parameter values are as follows: cell length $L_s = 10$ m, UAV minimum turning radius $R_{\min} = 200$ m, UAV speed when flying above river $V = 10$ m/s, sensor detection probability $g_s = 0.9$, number of training data points $N = 2000$, and initial number of Gaussian models $K = 9$, $\lambda_1 = 1$, and $\lambda_2 = 2$.

A. Coverage Search by GMM-AI

Fig. 7 shows the prior likelihood distribution map of target in Wulong river, which is generated randomly by combining series of exponential functions as well as small noise functions. It consists of several clusters attached with high value of probability. Fig. 8 illustrates the distribution map as well as the GMM results by 1-D representation. It is evident that GMM method can approximate the real distribution map well. With different number of UAVs ($N_u = 1, 2, 3, 4$), these extracted subregions are then prioritized and allocated, and the planned routes under no terminal time constraint are as shown in Fig. 9. With proper allocation and sequencing strategy, UAV prefers to detect the areas with higher value at the beginning, and

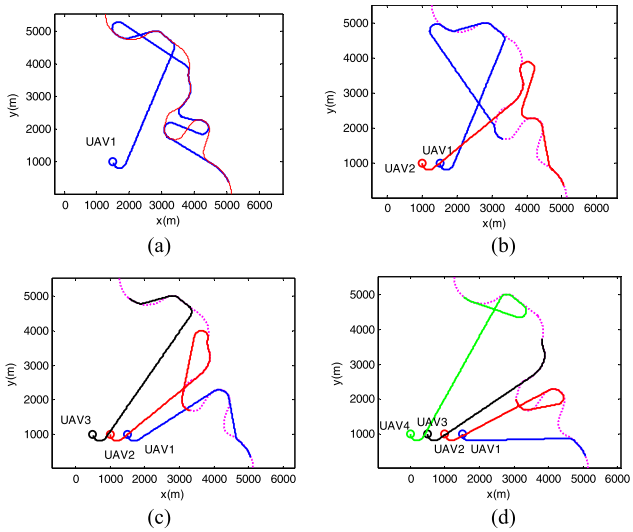

Fig. 9. Planned routes with different number of UAVs. (a) $N_u = 1$. (b) $N_u = 2$. (c) $N_u = 3$. (d) $N_u = 4$.

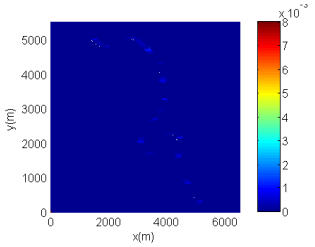

Fig. 10. Updated likelihood distribution map.

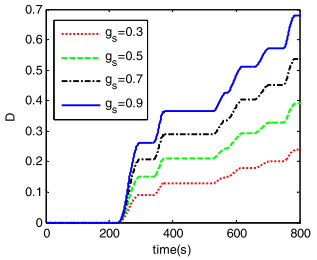

Fig. 11. Cumulative detection payoff with different g_s.

all the subregions will be covered eventually. Fig. 10 displays the updated likelihood distribution map by GMM-AI when the coverage search mission finishes. Compared with the prior map, the smaller values in the updated map indicate that the regions of interest are already detected.

The searching performance of single UAV with different sensor detection probabilities ($g_s = 0.3, 0.5, 0.7, 0.9$) is also analyzed. As shown in Fig. 11, the cumulative detection payoff increases with a higher g_s.

B. Comparison of Different Methods

To testify the advantages of GMM-AI, other four methods are utilized in the scenario of Section A as well for comparison. The first is full-sweeping method, and UAV will just fly along the river and completely cover the river after long time, as shown in Fig. 12(a). The second is greedy method, i.e., UAV first flies to the nearest river region directly and then sweeps the river in the direction of getting larger detection payoff,

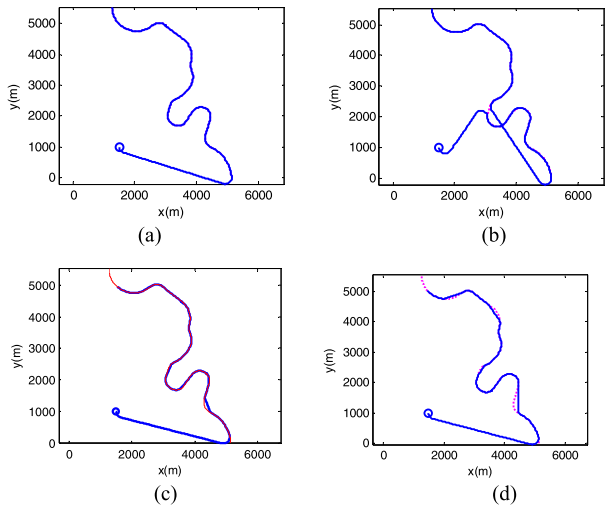

Fig. 12. Single-UAV path using different methods. (a) Full-sweeping method. (b) Greedy method. (c) Complete cell method. (d) GMM + RS.

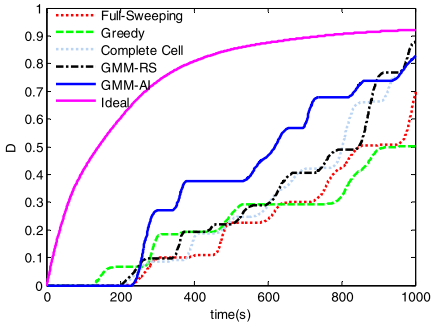

Fig. 13. Cumulative detection payoff by various methods.

as shown in Fig. 12(b). A conventional approach considering the complete set of real high-value and low-value cells (bigger than 0) along the river is employed for comparison, and the result is displayed in Fig. 12(c). When it comes to the fourth method, the subregions are also extracted by GMM, but visited by UAV in the random sequence (RS). Fig. 12(d) shows the route by GMM + RS, where UAV visits these river segments orderly for instance. Note that the route by complete cell method is similar to that by GMM + RS, but UAV will waste some time sweeping those low-value regions when the former method is used.

Due to the lack of heuristic principles, these four methods cannot guide UAV to visit the higher value subregions (upper left region) but get stuck in the lower valued ones in the early stage. Hence, the efficiency will certainly be unsatisfactory, especially when the mission time is short. Using GMM-AI method, however, UAV can search the river heuristically to collect the maximum payoff as soon as possible. Fig. 13 displays the curves of detection payoff versus time using different methods. The pink thick line denotes the reward of ideal route defined as follows: at each time, UAV jumps to the point attached with the maximum probability (nonadjacent to the last waypoint in most cases), ignoring UAV motion constraints. Hence, this curve is indeed the theoretical upper limit of detection reward. The payoff curve of GMM-AI is closest to the ideal curve in most stages (250–900 s), indicating its best performance with largest detection payoff, despite

TABLE I
FINAL PAYOFF BY VARIOUS METHODS

Method	400s	600s	800s	1000s
Full-Sweeping	0.1061	0.2375	0.4248	0.6903
Greedy	0.1919	0.2930	0.3202	0.5012
Complete Cell	0.1693	0.2890	0.4899	0.8380
GMM-RS	0.1929	0.2989	0.5020	**0.8701**
GMM-AI	**0.3772**	**0.4840**	**0.6610**	0.8272
Ideal path	0.8080	0.8752	0.9066	0.9217

TABLE II
COMPUTATION TIME BY VARIOUS METHODS (SECONDS)

Method	400s	600s	800s	1000s
Full-Sweeping	**0.01**	**0.01**	**0.02**	**0.03**
Greedy	0.02	0.02	0.03	0.03
Complete Cell	0.11	0.11	0.12	0.14
GMM-RS	1.75	1.74	1.79	1.76
GMM-AI	1.92	1.90	1.94	1.97

the exception that the greedy approach works best in the initial stage (130–250 s) and the payoff of GMM-RS is larger than GMM-AI in the final stage. Therefore, the advantage of GMM-AI is highlighted especially when the given mission time is short, and it is more applicable for time-sensitive search mission, where the higher value areas will be visited earlier. Table I shows the detection payoff by various methods as well as the ideal path under different mission times. The boldface of each column means the best result from all the methods. Similar to the above conclusion, GMM-AI method obtains the maximum payoff in most cases but is slightly worse than GMM-RS at 1000 s. Table II shows the computation time of various methods. All the methods have very small amount of calculation, although the running time by GMM-RS or GMM-AI is larger than others, where most effort actually focuses on extracting the river subregions by GMM. Overall the running time is still acceptable compared with the given mission time.

C. Statistical Results Using Different Methods

Using the five methods in Section B, the Monte Carlo experiments under different mission times (400, 600, 800, and 1000 s) are executed, respectively, each of which has 100 tests. In each test, the river environment or prior distribution is randomly generated by 5–20 exponential functions as well as corresponding noise functions. With the assumption $K = 9$ in the initial iteration of each test, the dynamic adaptive strategy is also used in GMM to automatically adapt to different scenarios.

The statistical results of final detection payoff including the minimum, mean, maximum, and SD are shown in Table III, where the best results of each column are marked with boldface. Our proposed GMM-AI method collects the maximum detection reward and has the minimum SD in most cases,

TABLE III
STATISTICAL RESULTS OF FINAL DETECTION PAYOFF

T_{given}(s)	Method	Minimum	Mean	Maximum	SD
400	Full-Sweeping	0.0882	0.1915	0.5970	0.1503
	Greedy	0.0452	0.1926	0.4421	0.1471
	Complete Cell	0.0995	0.2673	0.5507	0.1226
	GMM-RS	0.1200	0.2209	0.5644	0.1212
	GMM-AI	**0.1579**	**0.3793**	**0.6555**	**0.0968**
600	Full-Sweeping	0.1366	0.3088	0.6687	0.1142
	Greedy	0.0180	0.3263	0.4857	0.1341
	Complete Cell	0.1021	0.3295	0.5809	0.1088
	GMM-RS	0.1820	0.3736	0.5072	0.0994
	GMM-AI	**0.2043**	**0.3998**	**0.6764**	**0.0802**
800	Full-Sweeping	0.2203	0.4568	0.6737	0.1104
	Greedy	0.0850	0.4074	0.6632	0.1127
	Complete Cell	0.1895	0.4622	0.6901	0.0989
	GMM-RS	0.3972	0.4707	0.6800	0.0671
	GMM-AI	**0.5029**	**0.6404**	**0.7035**	**0.0426**
1000	Full-Sweeping	0.3608	0.5897	0.6863	0.0711
	Greedy	0.2177	0.4690	0.6744	0.0885
	Complete Cell	0.2773	0.5120	0.7004	0.0878
	GMM-RS	**0.6221**	0.6799	0.7110	**0.0348**
	GMM-AI	0.5836	**0.6840**	**0.7234**	0.0485

verifying its high efficiency and strong robustness to different scenarios.

V. CONCLUSION

Optimal UAV route planning for coverage search in a river region is studied, aiming to obtain the maximum probability of finding a lost target. Based on prior probability distribution map, river subregions are first extracted by GMM and then prioritized heuristically by AI. Besides, the positive/negative greedy method is presented to meet the terminal time constraint. With heuristic, the proposed GMM-AI method generates the optimal searching routes under constraints, and UAV prefers to detect the cluster areas attached with higher value of target probability in the early stage. Hence, it enables maximizing the cumulative detection payoff especially for the time-sensitive search mission. Simulation results show that GMM-AI has higher searching efficiency and stronger robustness to various scenarios compared with other methods. However, the lost target is assumed to be static in this brief, and the future work will focus on searching a mobile target.

REFERENCES

[1] R. W. Beard, T. W. McLain, D. B. Nelson, D. Kingston, and D. Johanson, "Decentralized cooperative aerial surveillance using fixed-wing miniature UAVs," *Proc. IEEE*, vol. 94, no. 7, pp. 1306–1324, Jul. 2006.

[2] K. Kalyanam, P. Chandler, M. Pachter, and S. Darbha, "Optimization of perimeter patrol operations using unmanned aerial vehicles," *J. Guid. Control Dyn.*, vol. 35, no. 2, pp. 434–441, 2012.

[3] H. Oh, S. Kim, H.-S. Shin, and A. Tsourdos, "Coordinated standoff tracking of moving target groups using multiple UAVs," *IEEE Trans. Aerosp. Electron. Syst.*, vol. 51, no. 2, pp. 1501–1514, Apr. 2015.

[4] Y. Wang, S. Wang, and M. Tan, "Path generation of autonomous approach to a moving ship for unmanned vehicles," *IEEE Trans. Ind. Electron.*, vol. 62, no. 9, pp. 5619–5629, Sep. 2015.

[5] F. Bourgault, T. Furukawa, and H. F. Durrant-Whyte, "Coordinated decentralized search for a lost target in a Bayesian world," in *Proc. IEEE/RSJ Int. Conf. Intell. Robots Syst.*, Oct. 2003, pp. 48–53.

[6] V. Roberge, M. Tarbouchi, and G. Labonte, "Comparison of parallel genetic algorithm and particle swarm optimization for real-time UAV path planning," *IEEE Trans. Ind. Informat.*, vol. 9, no. 1, pp. 132–141, Feb. 2013.

[7] P. Yao, H. Wang, and Z. Su, "UAV feasible path planning based on disturbed fluid and trajectory propagation," *Chin. J. Aeronaut.*, vol. 28, no. 4, pp. 1163–1177, 2015.

[8] E. Galceran and M. Carreras, "A survey on coverage path planning for robotics," *Robot. Auton. Syst.*, vol. 61, no. 12, pp. 1258–1276, 2013.

[9] F. Balampanis, I. Maza, and A. Ollero, "Area decomposition, partition and coverage with multiple remotely piloted aircraft systems operating in coastal regions," in *Proc. Int. Conf. Unmanned Aircraft Syst. (ICUAS)*, Jun. 2016, pp. 275–283.

[10] R. W. Beard and T. W. McLain, "Multiple UAV cooperative search under collision avoidance and limited range communication constraints," in *Proc. 42nd IEEE Conf. Decision Control*, Maui, HI, USA, Dec. 2003, pp. 25–30.

[11] M. Torres, D. A. Pelta, J. L. Verdegay, and J. C. Torres, "Coverage path planning with unmanned aerial vehicles for 3D terrain reconstruction," *Expert Syst. Appl.*, vol. 55, pp. 441–451, Aug. 2016.

[12] E. U. Acar, H. Choset, and J. Y. Lee, "Sensor-based coverage with extended range detectors," *IEEE Trans. Robot.*, vol. 22, no. 1, pp. 189–198, Feb. 2006.

[13] J. R. Riehl, G. E. Collins, and J. P. Hespanha, "Cooperative search by UAV teams: A model predictive approach using dynamic graphs," *IEEE Trans. Aerosp. Electron. Syst.*, vol. 47, no. 4, pp. 2637–2656, Oct. 2011.

[14] P. Lanillos, S. K. Gan, E. Besada-Portas, G. Pajares, and S. Sukkarieh, "Multi-UAV target search using decentralized gradient-based negotiation with expected observation," *Inf. Sci.*, vol. 282, pp. 92–110, Oct. 2014.

[15] J. Hu, L. Xie, K. Y. Lum, and J. Xu, "Multiagent information fusion and cooperative control in target search," *IEEE Trans. Control Syst. Technol.*, vol. 21, no. 4, pp. 1223–1235, Jul. 2013.

[16] M.-H. Kim, H. Baik, and S. Lee, "Response threshold model based UAV search planning and task allocation," *J. Intell. Robot. Syst.*, vol. 75, nos. 3–4, pp. 625–640, 2014.

[17] J. Berger and N. Lo, "An innovative multi-agent search-and-rescue path planning approach," *Comput. Oper. Res.*, vol. 53, pp. 24–31, Jan. 2015.

[18] P. Yao, H. Wang, and H. Ji, "Gaussian mixture model and receding horizon control for multiple UAV search in complex environment," *Nonlinear Dyn.*, vol. 88, no. 2, pp. 903–919, 2017.

[19] S. Rathinam *et al.*, "Autonomous searching and tracking of a river using an UAV," in *Proc. Amer. Control Conf.*, Jul. 2007, pp. 359–364.

[20] K. Savla, E. Frazzoli, and F. Bullo, "Traveling salesperson problems for the Dubins vehicle," *IEEE Trans. Autom. Control*, vol. 53, no. 6, pp. 1378–1391, Jul. 2008.

[21] H. Oh, S. Kim, A. Tsourdos, and B. A. White, "Coordinated road-network search route planning by a team of UAVs," *Int. J. Syst. Sci.*, vol. 45, no. 5, pp. 825–840, 2014.

[22] M. Dille and S. Singh, "Efficient aerial coverage search in road networks," in *Proc. AIAA Guid., Navigat., Control*, Aug. 2013, pp. 1–20, paper AIAA 2013-5094.

[23] W. Meng, Z. He, R. Su, P. K. Yadav, R. Teo, and L. Xie, "Decentralized multi-UAV flight autonomy for moving convoys search and track," *IEEE Trans. Control Syst. Technol.*, vol. 25, no. 4, pp. 1480–1487, Jul. 2017.

[24] M. Dille, B. Grocholsky, and S. Singh, "Guaranteed road network search with small unmanned aircraft," in *Proc. IEEE/RSJ Int. Conf. Intell. Robots Syst.*, Sep. 2014, pp. 4789–4796.

[25] V. Dobrokhodov *et al.*, "On coordinated road search using time-coordinated path following of multiple UAVs," in *Proc. AIAA Guid., Navigat., Control Conf.*, Aug. 2010, pp. 1–10, paper AIAA 2010-7583.

[26] K. Obermeyer, P. Oberlin, and S. Darbha, "Sampling-based roadmap methods for a visual reconnaissance UAV," in *Proc. AIAA Guid., Navigat., Control Conf.*, Aug. 2010, pp. 1–21, paper AIAA 2010-7568.

[27] A. Gruszka, M. Malisoff, and F. Mazenc, "Bounded tracking controllers and robustness analysis for UAVs," *IEEE Trans. Autom. Control*, vol. 58, no. 1, pp. 180–187, Jan. 2013.

[28] L. Lin and M. A. Goodrich, "Hierarchical heuristic search using a Gaussian mixture model for UAV coverage planning," *IEEE Trans. Cybern.*, vol. 44, no. 12, pp. 2532–2544, Dec. 2014.

[29] L. E. Dubins, "On curves of minimal length with a constraint on average curvature, and with prescribed initial and terminal positions and tangents," *Amer. J. Math.*, vol. 79, no. 3, pp. 497–516, 1957.

[30] D. J. Rosenkrantz, R. E. Stearns, and P. M. Lewis, II, "An analysis of several heuristics for the traveling salesman problem," in *Fundamental Problems in Computing*. Amsterdam, The Netherlands: Springer, 2009, pp. 45–69.